Analysis of Hopf Bifurcation in Parallel-Connected Boost Converters via Averaged Models

H. H. C. Iu, C. K. Tse, V. Pjevalica and Y.M. Lai

Department of Electronic and Information Engineering, Hong Kong Polytechnic University, Hong Kong

herbert@eie.polyu.edu.hk & cktse@eie.polyu.edu.hk

Abstract — This paper attempts to study the bifurcation phenomena of a system of parallel-connected dc/dc boost converters. In particular, it is shown that simple averaged models can be used to predict the occurrence of Hopf bifurcation in such systems. The results provide important information for the design of stable current sharing in a master-slave configuration.

I Introduction

Recently, paralleling converters has become a popular technique in power supply design for improving power capability, reliability and flexibility. The main design issue in parallel converters is the control of the sharing of current among the constituent converters. In practice, mandatory control is needed to ensure proper current sharing, and many effective control schemes have been proposed in the past [1]–[2]. One common approach is to employ an active control scheme to force the current in one converter to follow that of the other. Such a scheme is commonly known as the *master-slave* current-sharing scheme [1]–[2].

Bifurcation behaviour in dc/dc converter systems is usually studied via a discrete-time approach [3]–[4]. However, the mathematics involved is rather complicated when using such an approach. In this paper, we use a simple state-space averaged model to study some low-frequency nonlinear behaviour of a system of parallel-connected boost converters.

II Master-Slave Current-Sharing Controlled Parallel-Connected DC/DC Converters

The system under study consists of two dc/dc converters which are connected in parallel feeding a common load. Denoting the two converters as Converter 1 and Converter 2 as shown in Fig. 1, the operation of the system can be described as follows. Both converters are controlled via a simple pulse-width modulation (PWM) scheme, in which a control voltage $v_{\rm con}$ is compared with a sawtooth signal to generate a pulse-width modulated signal that drives the switch. The sawtooth signal of the PWM generator is

$$v_{\rm ramp} = V_L + (V_U - V_L)\frac{t \bmod T}{T}, \qquad (1)$$

where V_L and V_U are the lower and upper voltage limits of the ramp, and T is the switching period. The PWM output is "high" when the control voltage is greater than $v_{\rm ramp}$, and is "low" otherwise.

The control voltages of Converters 1 and 2 are given by the following equations:

$$v_{\rm con1} = V_{\rm offset} - K_{v1}(v - V_{\rm ref}) \qquad (2)$$

$$v_{\rm con2} = V_{\rm offset} - K_{v2}(v - V_{\rm ref}) - K_i(i_2 - i_1) \qquad (3)$$

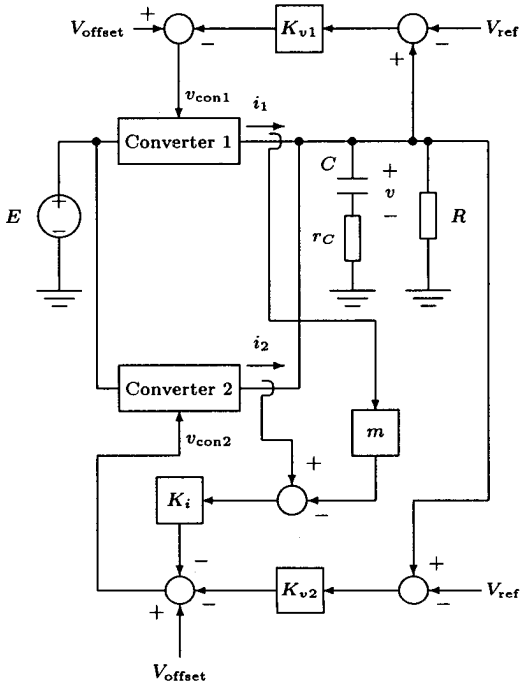

Fig. 1: Block diagram of parallel-connected dc/dc converters under a master-slave current-sharing control

where $V_{\rm offset}$ is a dc offset voltage that gives the steady-state duty cycle, $V_{\rm ref}$ is the reference voltage, K_{v1} and K_{v2} are the voltage feedback gains, K_i is the current feedback gain, and m is a current weighting factor. Under this scheme, the output current of both Converter 2 will follow that of Converter 1 at a ratio of m to 1, where $m > 0$. In this paper, we assume m=1. Converter 1 is commonly referred to as the "master" and Converter 2 the "slave" which imitates the master's current value.

III State-space Averaged Model for Two Parallel Boost Converters

Figure 2 shows two boost converters connected in parallel. The space-space averaged model for the parallel-connected boost converters is shown in Fig. 3. The system can be represented by the state-space averaged equations:

$$\begin{aligned}\frac{di_1}{dt} &= \frac{-(1-d_1)v}{L_1} + \frac{E}{L_1}\\ \frac{di_2}{dt} &= \frac{-(1-d_2)v}{L_2} + \frac{E}{L_2}\\ \frac{dv}{dt} &= \frac{(1-d_1)i_1}{C} + \frac{(1-d_2)i_2}{C} - \frac{v}{RC},\end{aligned} \qquad (4)$$

0-7803-7448-7/02/$17.00 ©2002 IEEE

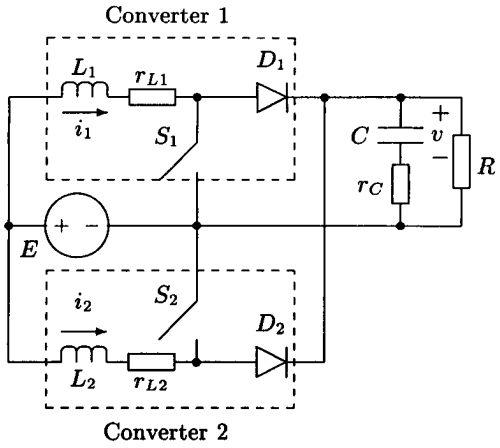

Fig. 2: Two parallel-connected boost converters

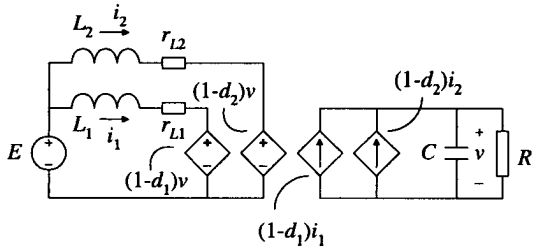

Fig. 3: The state-space averaged model of parallel-connected boost converters

where d_1 and d_2 are the duty cycles of Converter 1 and Converter 2 respectively. We assume that r_{L1}, r_{L2} and r_C are zero in order to simplify the subsequent analysis. The duty cycles d_1 and d_2 can be represented by:

$$d_1 = D - k_{v1}(v - V_{\text{ref}}), \tag{5}$$

$$d_2 = D - k_{v2}(v - V_{\text{ref}}) - k_i(i_2 - i_1), \tag{6}$$

where D is the steady-state duty cycle, $k_{v1} = \frac{K_{v1}}{V_U - V_L}$, $k_{v2} = \frac{K_{v2}}{V_U - V_L}$ and $k_i = \frac{K_i}{V_U - V_L}$. It should be noted that $0 < d_1 < 1$ and $0 < d_2 < 1$ should be satisfied. Putting (5) and (6) into (4), we get a set of autonomous equations that that can be further simplified in a dimensionless form.

We define the dimensionless state variables as follows:

$$x_1 = \frac{i_1 R}{V_{\text{ref}}}, \quad x_2 = \frac{i_2 R}{V_{\text{ref}}}, \quad x_3 = \frac{v}{V_{\text{ref}}}. \tag{7}$$

We also define the dimensionless time and parameters as follows:

$$\tau = \frac{t}{T}, \quad \xi_1 = \frac{L_1}{RT}, \quad \xi_2 = \frac{L_2}{RT}, \quad \zeta = \frac{CR}{T},$$

$$\kappa_{v1} = k_{v1}V_{\text{ref}}, \quad \kappa_{v2} = k_{v2}V_{\text{ref}}, \quad \kappa_i = \frac{k_i V_{\text{ref}}}{R}, \quad e = \frac{E}{V_{\text{ref}}}. \tag{8}$$

Direct substitution of these new dimensionless variables, time and parameters in (4), (5) and (6) yields the following dimensionless autonomous equations:

$$\begin{aligned}
\frac{dx_1}{d\tau} &= \frac{e - (1 - D + \kappa_{v1}(x_3 - 1))x_3}{\xi_1} \\
\frac{dx_2}{d\tau} &= \frac{e - (1 - D + \kappa_{v2}(x_3 - 1) + \kappa_i(x_2 - x_1))x_3}{\xi_2} \\
\frac{dx_3}{d\tau} &= \frac{(1 - D + \kappa_{v1}(x_3 - 1))x_1}{\zeta} \\
&\quad + \frac{(1 - D + \kappa_{v2}(x_3 - 1) + \kappa_i(x_2 - x_1))x_2 - x_3}{\zeta}.
\end{aligned} \tag{9}$$

We should note that (5) and (6) can be written as

$$d_1 = D - \kappa_{v1}(x_3 - 1), \tag{10}$$

$$d_2 = D - \kappa_{v2}(x_3 - 1) - \kappa_i(x_2 - x_1). \tag{11}$$

To complete the model, saturation must be included. When $d_1 < 0$ or/and $d_2 < 0$, we put $d_1 = 0$ or/and $d_2 = 0$ in (4) and perform dimensionless substitution. Similarly, when $d_1 > d_{\max}$ or/and $d_2 > d_{\max}$, we put $d_1 = d_{\max}$ or/and $d_2 = d_{\max}$ in (4) and perform dimensionless substitution ($d_{\max} < 1$ since the duty cycle of the boost converter cannot be equal to 1 exactly in practice).

The equilibrium point can be calculated by setting all time-derivatives in (9) to zero and solve for x_1, x_2 and x_3. This gives

$$X = \begin{bmatrix} X_1 \\ X_2 \\ X_3 \end{bmatrix} = \begin{bmatrix} \frac{1}{2e} \\ \frac{1}{2e} \\ 1 \end{bmatrix}. \tag{12}$$

IV Stability of Equilibrium Point and Hopf Bifurcation

The Jacobian, $J(X)$, for the dimensionless system evaluated at the equilibrium point is given by

$$J(X) = \begin{bmatrix} 0 & 0 & \frac{-(\kappa_{v1}+1-D)}{\xi_1} \\ \frac{\kappa_i}{\xi_2} & \frac{-\kappa_i}{\xi_2} & \frac{-(\kappa_{v2}+1-D)}{\xi_2} \\ \frac{2e(1-D)-\kappa_i}{2e\zeta} & \frac{2e(1-D)+\kappa_i}{2e\zeta} & \frac{\kappa_{v1}+\kappa_{v2}-2e}{2e\zeta} \end{bmatrix}. \tag{13}$$

We attempt to study the stability of the equilibrium point and the trajectory in the neighbourhood of the equilibrium point by deriving the eigenvalues of the system at the equilibrium point. The usual procedure is to solve the following equation for λ:

$$\det[\lambda \mathbf{1} - J(X)] = 0. \tag{14}$$

Using the above equation, the following conditions are easily verified:

$$\lim_{\lambda \to -\infty} \det[\lambda \mathbf{1} - J(X)] \to -\infty, \tag{15}$$

$$\det[-J(X)] > 0. \tag{16}$$

Hence, there exists at least one $\lambda \in (-\infty, 0)$ such that $\det[\lambda \mathbf{1} - J(X)] = 0$, i.e., the system has at least one negative real eigenvalue. Also, numerical calculations of eigenvalues for the practical range of parameters reveal that the other two eigenvalues are a complex conjugate pair which have either a positive or negative real part depending upon values of κ_{v1} and κ_{v2}. In particular, the following observations are made.

For small values of κ_{v1} and κ_{v2}, the pair of eigenvalues has a negative real part. As κ_{v1} or/and κ_{v2} increases, the real part of the complex eigenvalues get less negative, and at a critical value of κ_{v1} or/and κ_{v2}, the real part changes from negative to positive. The loci of the complex eigenvalue pair are plotted in Fig. 4. The critical value of κ_{v1} or/and κ_{v2} depends on the values of ξ_1, ξ_2, ζ, e and κ_i. As we increase κ_{v1} or/and κ_{v2}, the sign of the real part of the complex eigenvalues changes, the system loses stability via a *Hopf bifurcation* [5].

V Local Trajectories from the Averaged Equations

In this section, we re-examine the stability in terms of the local trajectories near the equilibrium point. Since the use of an

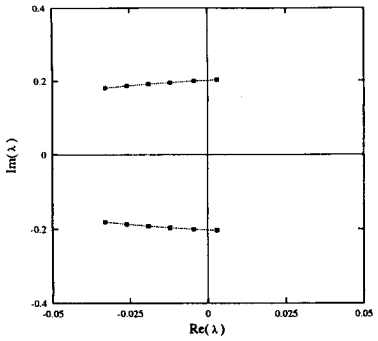

Fig. 4: Loci of the complex eigenvalue pair moving from left to right as K_{v2} is increased

averaged model for predicting nonlinear phenomena will become inadequate when stability is lost, our aim in this section is to observe, by plotting the local trajectories, the behaviour of the system as it goes from a stable region to an unstable region. For further investigation beyond the bifurcation point predicted by the averaged model, we need to resort to the exact piecewise switched model, as will be reported in the next section.

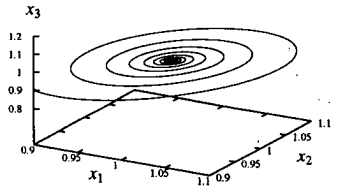

Fig. 5: View of the stable (spiralling inward) local trajectory based on the averaged model.

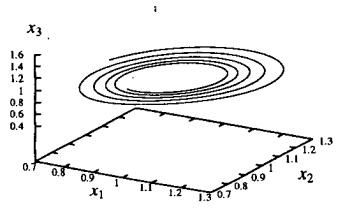

Fig. 6: View of the unstable (spiralling outward) local trajectory based on the averaged model.

The trajectory of the system near the equilibrium point can be easily derived from the corresponding eigenvalues and eigenvectors. We will illustrate two typical local trajectories, corresponding to a stable and an unstable equilibrium point. We first examine the stable system with κ_{v1}=0.48, κ_{v2}=0.45 and κ_i=0.40. The trajectory is shown in Fig. 5. We next examine the unstable system with κ_{v1}=0.48, κ_{v2}=0.55 and κ_i=0.40. The system loses stability and the trajectory is shown in Fig. 6. From the above trajectories, we clearly observe that the system loses stability via a Hopf bifurcation.

VI Computer Simulation Study

As the averaged continuous model falls short of predicting the details after the bifurcation, we examine the system again using computer simulation which employs an exact piecewise switched model. The following circuit parameters are used in our simulations: switching period T=40μs, input voltage E=24V, output voltage v=24V, inductance L_1=0.004H, r_{L1}=0.05Ω, inductance L_2=0.004H, r_{L2}=0.2Ω, capacitance C=10μF, r_C= 0.01Ω and load resistance R= 10Ω.

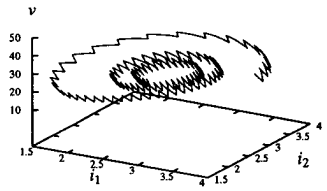

Fig. 7: View of the stable (spiralling inward) local trajectory based on the exact piecewise switched model.

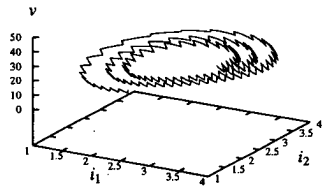

Fig. 8: View of the unstable (spiralling outward) local trajectory based on the exact piecewise switched model.

Since we are simulating the actual circuits, the original circuit parameters will be used instead of the dimensionless ones. In particular we will focus on the qualitative change of dynamics as K_{v1} or/and K_{v2} is varied. To observe the trend, we keep K_{v1} constant and vary K_{v2} (similar trend is observed when we keep K_{v2} constant and vary K_{v1}).

When K_{v2} is small, the trajectory spirals into a fixed period-1 orbit, corresponding to a fixed point in the averaged system. Figure 7 shows the simulated trajectory. When K_{v2} is increased beyond a critical value, the period-1 orbit becomes unstable, and the trajectory spirals outward as shown in Fig. 8. These observations confirm the prediction we made in Section V based on the averaged equations.

In order to give a better view of the system dynamics after the Hopf bifurcation, a large number of trajectories and bifurcation diagrams have been obtained. In the following, only representative bifurcation diagrams and sequence of trajectories are shown, which serve to exemplify the main findings concerning the bifurcation behaviour of a system of parallel boost converters under a master-slave current sharing scheme.

We first keep K_{v1} constant and vary K_{v2}. A bifurcation diagram is shown in Fig. 9(a). The sequence of simulated trajectories, as shown in Figs. 9(b), (c) and (e), reveals a typical Hopf bifurcation in which a stable equilibrium state breaks down to quasi-periodic orbits and limit cycles. The corresponding stroboscopic maps showing a quasi-periodic orbit and a limit cycle are shown in Figs. 9(d) and (f). Next, we keep K_{v2} constant and vary K_{v1}. Similar bifurcation diagram and trajectories are obtained. For brevity, they are not repeated here.

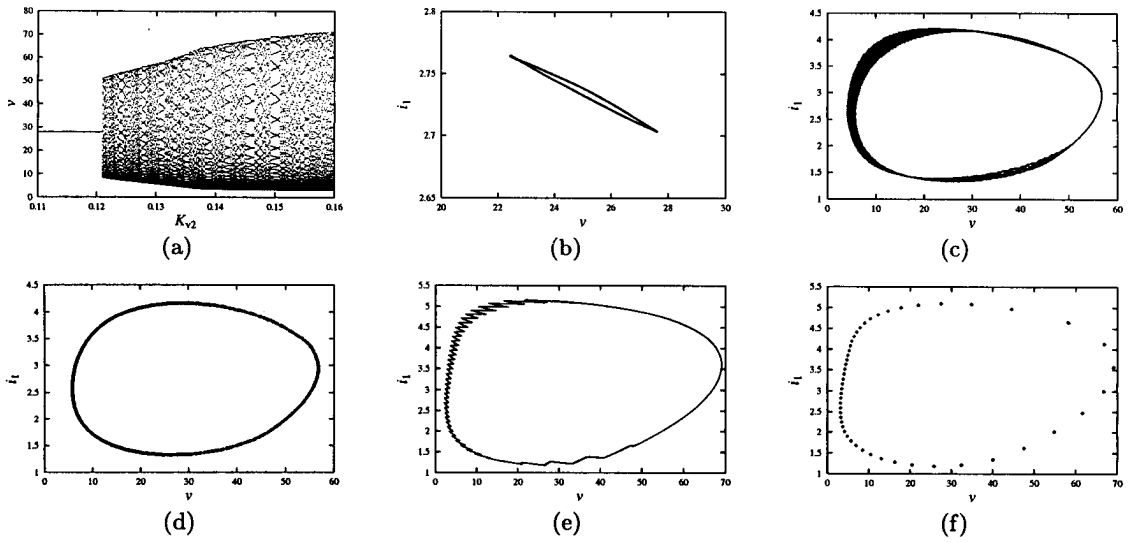

Fig. 9: (a) Bifurcation diagram with K_{v2} as bifurcation parameter ($K_{v1} = 0.11$ and $K_i = 1$); (b) Stable period-1 orbit ($K_{v1} = 0.11$, $K_{v2} = 0.11$ and $K_i = 1$); (c) Quasi-periodic orbit ($K_{v1} = 0.11$, $K_{v2} = 0.13$ and $K_i = 1$); (d) Stroboscopic map of (c); (e) Limit cycle ($K_{v1} = 0.11$, $K_{v2} = 0.15$ and $K_i = 1$); (f) Stroboscopic map of (e)

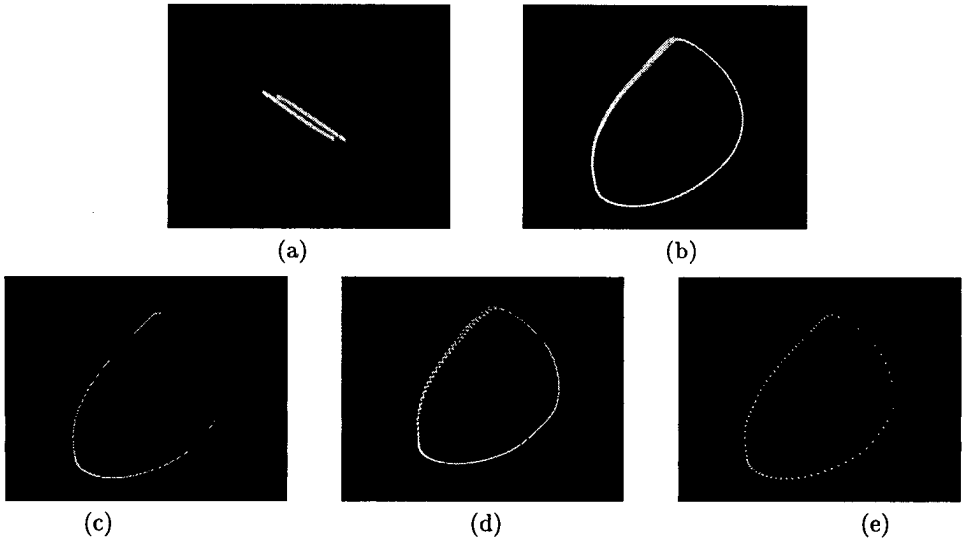

Fig. 10: Sequence of changes observed experimentally when K_{v2} is increased. (a) Stable period-1 orbit; (b) Quasi-periodic orbit; (c) Stroboscopic map of (b); (d) Limit cycle; (e) Stroboscopic map of (d). (Horizontal scale: 5V/div, vertical scale: 0.04A/div for (a); Horizontal scale: 10V/div, vertical scale: 0.4A/div for (b)—(e).)

VII Experimental Verification

We build a circuit to verify our simulation results. As we increase K_{v2}, we get results which are in good agreement with our simulations. The Hopf bifurcation takes place at approximately the same location (in terms of the value of the dc gain) as it does in our simulations. Trajectories of stable period-1 orbit, quasi-periodic orbit and limit cycle are captured, along with stroboscopic maps showing quasi-periodic orbits and limit cycles. Figures 10(a)–(e) show the sequence of changes when we increase K_{v2}. Figure 10(a) shows a stable period-1 orbit. Figure 10(b) shows a quasi-periodic orbit and Fig. 10(c) gives its the stroboscopic map. Figure 10(d) shows a limit cycle and Fig. 10(e) gives its the stroboscopic map.

VIII Conclusion

This paper attempts to use a simple state-space averaged model to explain some low-frequency nonlinear behaviour in a parallel system of two boost converters which share current under a master-slave control scheme. It has been found that Hopf bifurcation is possible when the voltage feedback gains are varied. These results are useful for practical design of such systems.

References

[1] V.J. Thottuvelil and G.C. Verghese, "Analysis and control of paralleled dc/dc converters with current sharing," *IEEE Trans. Power Electron.*, Vol. 13, No. 4, pp. 635–644, Jul 1998.

[2] Y. Panov, J. Rajagopalan and F.C. Lee, "Analysis and design of N paralleled DC-DC converters with master-slave current-sharing control," *IEEE Appl. Power Electron. Conf. Rec.*, pp. 436–442, 1997.

[3] H.H.C. Iu and C.K. Tse, "Bifurcation behaviour in parallel-connected buck converters," *IEEE Trans. Circ. Syst. Part I*, Vol. 48, No. 2, pp. 233–240, Feb 2001.

[4] H.H.C. Iu, C.K. Tse, V. Pjevalica and Y.M. Lai "Bifurcation behaviour in parallel-connected boost converters," *Int. J. Circuit Theory Appl.*, Vol. 29, No. 3, pp. 281–298, May 2001.

[5] K.T. Alligood, T.D. Sauer and J.A. Yorke, *Chaos: An Introduction to Dynamical Systems,* New York: Springer-Verlag, 1996.